Since January 2020 Elsevier has created a COVID-19 resource centre with free information in English and Mandarin on the novel coronavirus COVID-19. The COVID-19 resource centre is hosted on Elsevier Connect, the company's public news and information website.

Tuberculosis 107 (2017) 126–132

Contents lists available at ScienceDirect

Tuberculosis

journal homepage: http://intl.elsevierhealth.com/journals/tube

MODEL SYSTEMS

Modeling tuberculosis pathogenesis through *ex vivo* lung tissue infection

Pilar Carranza-Rosales [a], Irma Edith Carranza-Torres [a, b], Nancy Elena Guzmán-Delgado [c], Gerardo Lozano-Garza [a], Licet Villarreal-Treviño [b], Carmen Molina-Torres [d], Javier Vargas-Villarreal [a], Lucio Vera-Cabrera [d], Jorge Castro-Garza [a, *]

[a] Centro de Investigación Biomédica del Noreste, Instituto Mexicano del Seguro Social, 2 de Abril 501 ote, Col. Independencia, 64720, Monterrey, N.L., Mexico
[b] Departamento de Microbiología, Facultad de Ciencias Biológicas, Universidad Autónoma de Nuevo León, Avenida Pedro de Alba y Manuel L, Barragán s/n, Cd. Universitaria, 66450, San Nicolás de los Garza, N.L., Mexico
[c] Departamento de Patología, Unidad Médica de Alta Especialidad # 34, Instituto Mexicano del Seguro Social, Monterrey, N.L. 64730, Mexico
[d] Servicio de Dermatología, Hospital Universitario "José E. González", Universidad Autónoma de Nuevo León, Madero y Gonzalitos, Col. Mitras Centro, Monterrey, N.L., Mexico

ARTICLE INFO

Article history:
Received 3 April 2017
Received in revised form
6 September 2017
Accepted 10 September 2017

Keywords:
Mycobacterium tuberculosis
Lung
Tissue slices
Pathogenesis

ABSTRACT

Tuberculosis (TB) is one of the top 10 causes of death worldwide. Several *in vitro* and *in vivo* experimental models have been used to study TB pathogenesis and induction of immune response during *Mycobacterium tuberculosis* infection. Precision cut lung tissue slices (PCLTS) is an experimental model, in which all the usual cell types of the organ are found, the tissue architecture and the interactions amongst the different cells are maintained. PCLTS in good physiological conditions, monitored by MTT assay and histology, were infected with either virulent *Mycobacterium tuberculosis* strain H37Rv or the TB vaccine strain *Mycobacterium bovis* BCG. Histological analysis showed that bacilli infecting lung tissue slices were observed in the alveolar septa, alveolar light spaces, near to type II pneumocytes, and inside macrophages. Mycobacterial infection of PCLTS induced TNF-α production, which is consistent with previous *M. tuberculosis in vitro* and *in vivo* studies. This is the first report of using PCLTS as a system to study *M. tuberculosis* infection. The PCLTS model provides a useful tool to evaluate the innate immune responses and other aspects during the early stages of mycobacterial infection.

1. Introduction

Mycobacterium tuberculosis, the primary cause of human tuberculosis (TB), has infected one third of all humanity, and it is a leading cause of death by a single infectious agent [1].

Diverse approaches have been used to study TB pathogenesis. Discovery of mechanisms of adherence, infection routes, secreted or contact-dependent bacterial factors, evasion of immune response, signaling, and dissemination in tissues have been possible using *in vitro* and *in vivo* models. Such studies can reveal useful information to aid in the development of products or strategies to prevent or treat TB. Both, *in vitro* as well as *in vivo* experimental systems have advantages and limitations. Each has become complementary to the other to dissect the pathogenic mechanisms of microorganisms and host immune response.

An alternative model, bridging *in vivo* and *in vitro*, is an *ex vivo* model that uses original tissue explants: the precision cut lung tissue slices (PCLTS). In this system, all of the typical cell types of the organ are found, the tissue architecture and interactions between the different cells are maintained, and metabolic and transport functions are preserved [2].

Lung tissue slices have been used for toxicity studies [3], biotransformation [4], metabolism of xenobiotics [5], and to study infectious agents like coronavirus [6], retrovirus [7], influenza and parainfluenza viral strains [2,8–12], viruses of the bovine respiratory disease complex [13,14], respiratory syncytial virus (RSV), and only one bacteria *Chlamydophila pneumonia* [15]. These reports

* Corresponding author.
E-mail addresses: pilarcarranza@cibinmty.net (P. Carranza-Rosales), mitzba@hotmail.com (I.E. Carranza-Torres), nancyegd@gmail.com (N.E. Guzmán-Delgado), hglgarza@hotmail.com (G. Lozano-Garza), sporothrix@hotmail.com (L. Villarreal-Treviño), carmelia7@hotmail.com (C. Molina-Torres), jvargas147@yahoo.com.mx (J. Vargas-Villarreal), luvera_99@yahoo.com (L. Vera-Cabrera), jorgecg@yahoo.com (J. Castro-Garza).

http://dx.doi.org/10.1016/j.tube.2017.09.002
1472-9792/

show that lung tissue slices can be used in modeling different aspects of infection processes by various pathogens.

In the current study, we have optimized PCLTS for use as an alternative model to study mycobacterial infection in lung tissue.

2. Material and methods

2.1. Bacterial strains and growth conditions

M. tuberculosis strain H37Rv and *M. bovis* BCG were cultured in Middlebrook 7H9 broth supplemented with oleic acid/albumin/dextrose/catalase (OADC), grown to mid-logarithmic phase, and stored at −70 °C until needed. Bacterial titers for each batch of frozen stocks were determined in triplicate by colony-forming units (CFU) counting on Middlebrook 7H10 agar.

Before infection experiments, aliquots of bacterial stocks were thawed at 37 °C, mixed vigorously by vortexing, and diluted in tissue-culture medium to provide inocula to achieve the Multiplicity of Infection (MOI) indicated. MOI was confirmed from these preparations by CFU counting on Middlebrook 7H10 agar for each experiment.

2.2. Precision cut lung tissue slices preparation

PCLTS were prepared from 18 to 20 weeks old male BALB/c mice (*Mus musculus*) (Harlan Mexico). Mice were euthanized by cervical dislocation following institutional and international guidelines for humanitarian care of animals used in experimental work. Then pleural cavity was exposed under aseptic conditions and trachea was cannulated to infiltrate the lungs with 0.7% low-gelling temperature agarose in RPMI 1640 medium at 37 °C. Tissues were allowed to cool with ice to obtain an appropriately-firm consistency to cut the slices and the lungs were excised and immersed in sterile Krebs-Henseleit (KB) buffer (pH 7.4 at 4 °C).

Five millimeter diameter cores of lung tissue were obtained and then the cores were cut with a Brendel Vitron tissue slicer (Vitron, Tucson, AZ, USA) in oxygenated KB buffer (4 °C, 95:5% O_2:CO_2) into 350–400 μm thick tissue slices.

PCLTS were transferred into 24-well microplates (one per well) with 1 ml of DMEM/F12 medium supplemented with 10% bovine fetal serum and 25 mM glucose. PCLTS were incubated at 37 °C and 5% CO_2 in an orbital shaker (~40 rpm). After 1 h, medium was changed every 30 min to remove agarose.

Viability of PCLTS was determined by tetrazolium dye MTT (3-(4,5-Dimethylthiazol-2-yl)-2,5-Diphenyltetrazolium Bromide) assay in 24 well plates [16]. OD_{570nm} values were read in a microplate reader (Synergy HT, Biotek, Winooski, VT, USA). Viability of PCLTS was 95% at 72 h (data not shown).

2.3. Infection of PCLTS

Immediately after the last wash to remove agarose, the PCLTS were infected with 1.8×10^6 bacterial inoculum in 300 μl applied on top of the slices. Infected lung slices were incubated stationary for 1 h to facilitate adherence and infection. Then, 700 μl of complete DMEM/F12 medium was added to each well and the microplates were incubated at 37 °C and 5% CO2 in an orbital shaker (~40 rpm) for different infection periods. CFU were determined by plating in triplicate on Middlebrook 7H10 agar at each time point.

2.4. Histopathological analysis

After the indicated infection times, PCLTS were fixed with buffered formalin (10% in PBS) at 4 °C for 24 h to inactivate the mycobacteria [17]. A different microplate was used for each time point to avoid formaldehyde vapors from affecting other slice cultures. Infected and control slices were embedded in paraffin using an automated tissue processor (Citadel 1000, Shandon, Pennsylvania, USA). Sections of 5 μm thickness were obtained from the embedded tissues using a microtome (Vitron Inc, Tucson, AZ). The sections were stained with hematoxylin & eosin (H&E) or Ziehl-Neelsen (Z-N) dyes and visualized under a conventional light microscope.

2.5. RNA extraction and cDNA synthesis

At each time point, uninfected and infected PCLTS were transferred into RNAlater® solution, kept at 4 °C for 12 h, and then stored at −20 °C. RNA was extracted from all the samples at the same time using the RNeasy® Protect Mini kit (Qiagen) following manufacturer instructions. Quantity and purity of RNA were determined using a NanoDrop Spectrophotometer ND-1000 (Thermo Scientific, Massachusetts, USA). Integrity of RNA was visualized in agarose gels (1.5%) under denaturing conditions. Reverse transcription was performed using the ImProm-II Reverse Transcription System from Promega® (Madison, Wisconsin, USA) with random hexamers following manufacturer instructions. The generated cDNA was stored at −20 °C until used.

2.6. Analysis of TNF-α expression

Quantitative PCR assays for TNF-α were carried on by using TaqManÂ® Gene Expression Assays labeled with FAM™ (Dye/MGB Probe) from Applied Biosystems. As endogenous gene expression control, the murine GAPDH gene labeled with VIC (Dye/MGB Probe) was used. Each reaction mix contained 12.5 μl of TaqMan® Universal PCR Master Mix (2×), 1.25 μl of TaqMan® Gene Expression Assay (20×) Mix, 3 μl of cDNA (100 ng/μl) and 11.7 μl of nuclease-free water for a final volume of 25 μl. PCR was run in a 7500 Real Time PCR System from Applied Biosystems using the following parameters: (1) 50 °C for 2 min, (2) 95 °C for 10 min, and (3) 95 °C for 15 s, then 60 °C for 1 min; step 3 was repeated 40 times. Cycle threshold (C_T) data were exported to Excel to calculate expression levels comparing infected vs infected tissue lung slices at the same time point by $\Delta\Delta C_T$ method using the following equation:

$$\Delta\Delta C_T, = (\text{mean } C_{T,\ TNF\alpha \text{ gene, infected}} - \text{mean } C_{T,\ GAPDH \text{ gene, infected}}) - (\text{mean } C_{T,\ TNF\alpha \text{ gene, uninfected}} - \text{mean } C_{T,\ GAPDH \text{ gene, uninfected}})$$

$2^{-\Delta\Delta CT}$ = Expression of target gene in infected lung slices compared to the expression of target gene in uninfected lung slices for each time point.

Then, an ANOVA analysis using the Dunnett's method ($p < 0.05$) for comparison of means was performed to determine significance of values at the different time points.

3. Results

3.1. Histopathological analysis

Histopathological analysis of BALB/c mouse PCLTS by H & E staining showed that uninfected lung tissue slices maintained normal tissue architecture with no evidence of tissue damage up to 5 days of culture (Fig. 1). In infected PCLTS, at 24 h after infection, there was an increase in lymphocytes in areas where bacilli were located (Fig. 2). Mycobacteria infected PCLTS showed a mild inflammatory response characterized by the presence of lymphocytes, macrophages and multinucleated cells.

Fig. 3 show PCLTS sections infected with *M. tuberculosis* H37Rv or *M. bovis* BCG at different time points (0–48 h). *M. bovis* BCG

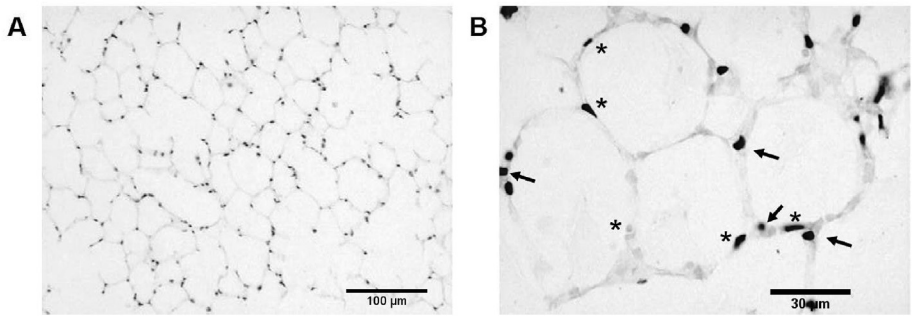

Fig. 1. Histological analysis of murine precision cut lung tissue slices (PCLTS) by H & E staining. At day 5 of culture, PCLTS show typical and well-preserved lung tissue structure; alveolar space are delimited by fine alveolar septa (1A, 100× magnification), pneumocytes type I (asterisks) are observed as squamous epithelial cells and pneumocytes type II as cuboidal cells (arrows) at the angles where alveolar septal walls converge (1B, 400× magnification).

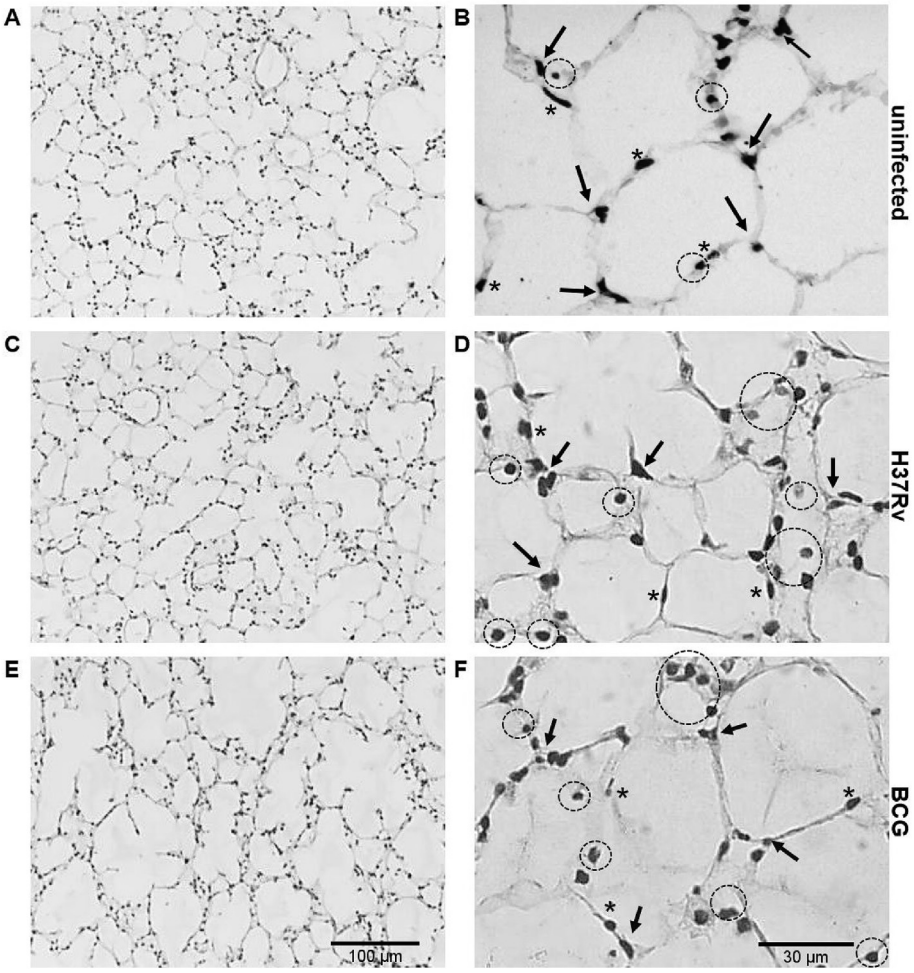

Fig. 2. H & E stained PCLTS after 24 h mycobacterial infection. Panels A and B correspond to lung tissue from uninfected PCLTS. Alveolar septa, pneumocytes type I (asterisk) and pneumocytes type II (arrow heads) are evident (panel B). Panels C and D correspond to *M. tuberculosis* H37Rv-infected PCLTS, while panels E and F to *M. bovis* BCG-infected PCLTS. In mycobacteria-infected PCLTS, there is an increase of inflammatory response predominantly lymphocytic (circles) (panels D and F). Magnification: 100× (A, C, and E) or 400× (B, D, and F).

bacilli were mainly located as free bacilli in the alveolar spaces and sometimes near type II pneumocytes. *M. tuberculosis* bacilli were located nearer to alveolar septa and near or in contact with type II pneumocytes.

Mycobacteria-infected PCLTS showed bacilli in the alveolar spaces with a tendency to group in the alveolar septum, near to or in contact with epithelial cells, but no bacteria were seen within pneumocytes. Meanwhile, intracellular bacteria were observed inside macrophages (Fig. 4). Presence of multinucleated giant cells and inflammatory cell aggregates, characteristic of a granulomatous disease like tuberculosis, were also frequently seen (Fig. 4).

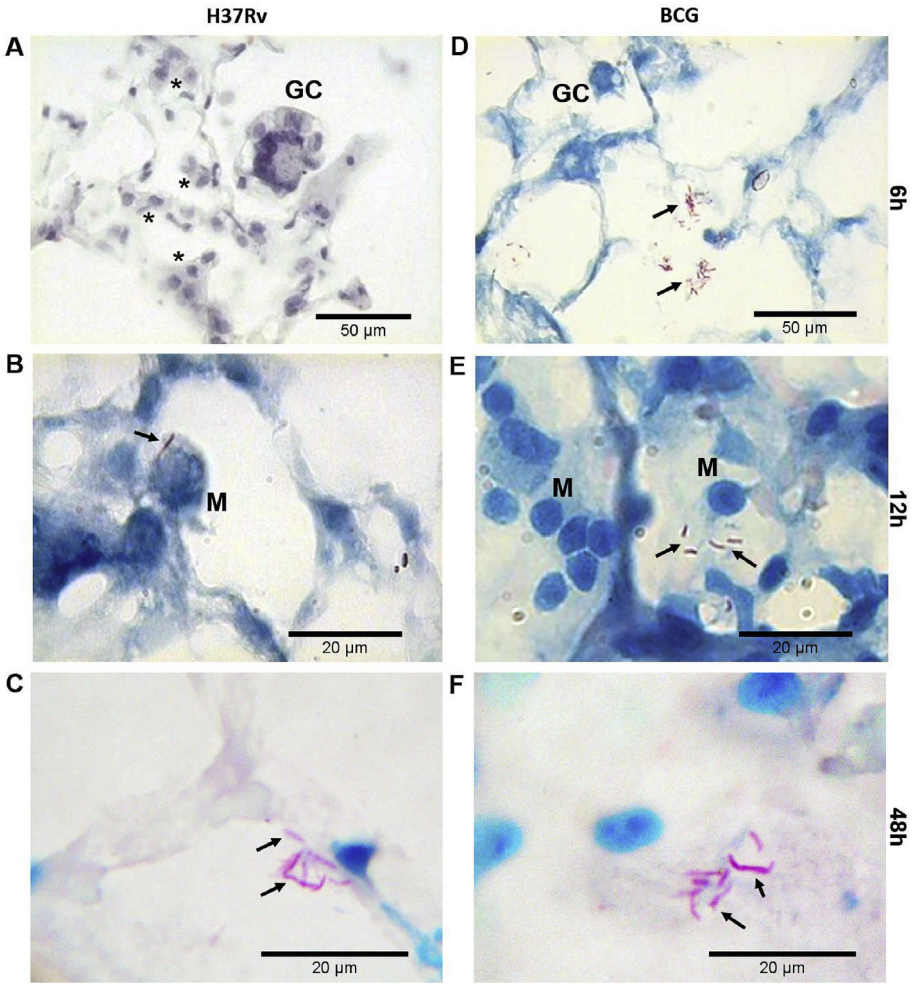

Fig. 3. Acid-fast staining of PCLTS infected with mycobacteria. PCLTS infected with *M. tuberculosis* H37Rv (A, B, and C) and *M. bovis* BCG (D, E, and F) at different time points. Multinucleated giant cells (GC), and lymphoplasmacytic infiltrate (asterisks) were evident. Mycobacterial aggregates were seen in the intra-alveolar space (arrows) interacting with macrophages (M), although the bacilli were primarily located near pneumocytes type II and alveolar septa. Staining: H&E (A), Ziehl-Neelsen (B, C, D, E and F). Magnification: 100× (A and D), and 1000× (B, C, E and F).

3.2. Mycobacteria CFU in PCLTS

Table 1 shows the CFU of both *M. tuberculosis* H37Rv and *M. bovis* BCG in PLCTS at different time points. There were not statically differences in number of CFU per slice.

3.3. TNF-α expression in infected lung slices

Comparison of TNF-α induction by mycobacteria infection by the ΔΔCt method indicated that TNF-α expression was higher in lung tissue slices infected with *M. bovis* BCG than in infected lung slices infected with *M. tuberculosis*. The peak of expression was at 6 h with *M. tuberculosis* producing an increase of 2.62 fold and *M. bovis* BCG increasing 3.38 fold (Fig. 5). Results of Dunnett's analysis of TNF-α gene expression are statistically significant for *M. bovis* BCG at 2, 6, 12 and 24 h and *M. tuberculosis* at 6 h compared to control values (Fig. 5).

4. Discussion

Despite all of the recent *M. tuberculosis* studies, there remain many unknown mechanisms associated with the tuberculosis pathogenesis due to the complex interactions between mycobacteria and host cells. Several *in vivo* and *in vitro* models have been useful to obtain information on different aspects of tuberculosis disease initiation and progression. Both types of models have advantages and weaknesses and in the end, they have become complementary to each other as sources of valuable data on *M. tuberculosis* virulence factors as well as on host immune responses to the pathogen. Here, we present an alternative and complementary *ex vivo* model using murine precision cut lung tissue slices to study *M. tuberculosis* infection. In this system all the usual cell types of the lung are present, the tissue architecture is maintained, as are the interactions between the different cells, and also important, the metabolic and transport functions are preserved. Additionally, at present it is virtually impossible to stop using animals in research and in a support for the moral and ethical issues handling experimental animals, this model reduces the number of animals used by experiment.

The main target organ for *M. tuberculosis* infection is the lung; therefore, respiratory tissue is the obvious first choice to evaluate PCLTS to study *M. tuberculosis* interactions with lung cells. Harford and Hamlin [18], prepared murine tissue slices by hand and reported the lung slices as an infection model for influenza virus, confirming the good physiological condition of the tissue by the presence of active ciliary movement. The first report on precision

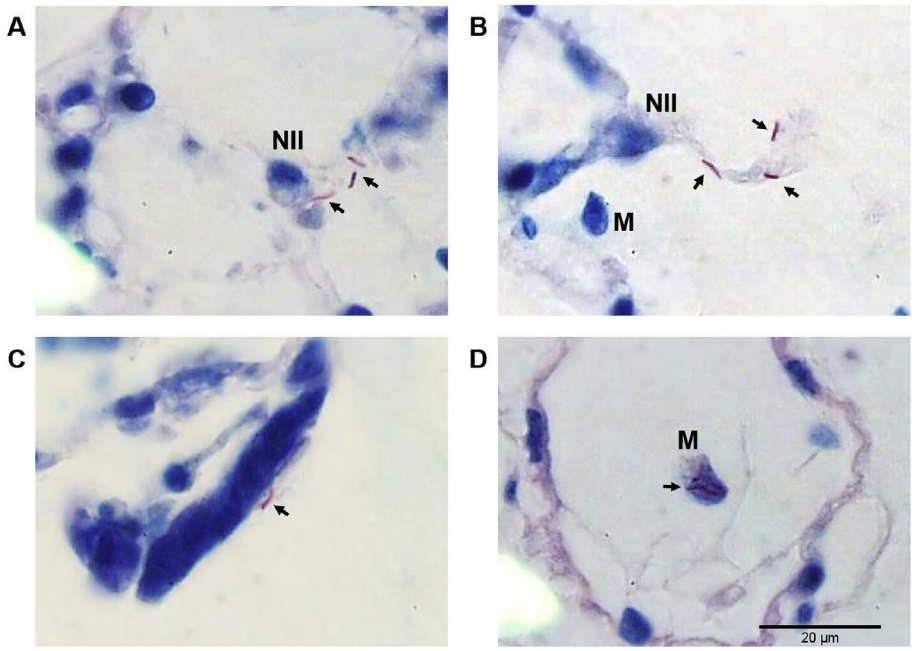

Fig. 4. Acid-fast staining of PCLTS infected with *M. tuberculosis* at 24 h post infection. Bacteria (arrows) are in contact with pneumocytes type II (NII) (panel A). Bacilli are also localized near alveolar septa and a macrophage is detected in the lumen of the alveolus (panel B). It was common to find mycobacteria on the surface of the epithelium (panel C) and inside alveolar macrophages (panel D). All sample were Ziehl-Neelsen stained. Magnification: 1000×.

Table 1
Mycobacterial CFU in PLCTS. Differences in number of CFU per slice were not statistically significant. Data represent the average of mycobacteria per slice ±standard deviation. Experiments were performed in triplicate.

	2 h	6 h	12 h	24 h
M. tuberculosis H37Rv	$1.12 \pm 0.19 \times 10^4$	$1.50 \pm 0.19 \times 10^4$	$2.10 \pm 0.32 \times 10^4$	$2.14 \pm 0.19 \times 10^4$
M. bovis BCG	$1.33 \pm 0.27 \times 10^4$	$1.64 \pm 0.38 \times 10^4$	$2.30 \pm 0.30 \times 10^4$	$2.35 \pm 0.25 \times 10^4$

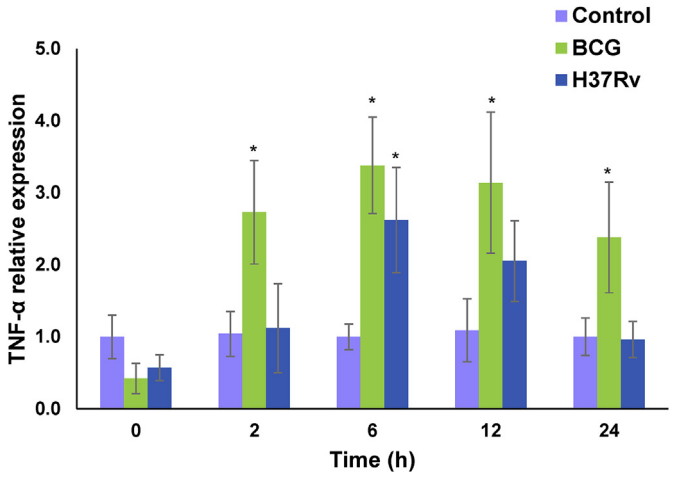

Fig. 5. TNF-α expression in PCLTS infected with mycobacteria. Bars show levels of relative TNF-α expression. Uninfected PCLTS (purple), *M. bovis* (green) or *M. tuberculosis* (blue) infected PCLTS. (For interpretation of the references to colour in this figure legend, the reader is referred to the web version of this article.)

cut lung slices was a study published by Ebsen et al. [15], in which lung slices were infected with *Chlamydophila pneumoniae* and respiratory syncytial virus. By using morphological analyses, these authors demonstrated that bacterial and viral infections can be successfully performed in this system.

Researchers have also infected PCLTS with different viruses (retrovirus, influenza virus and parainfluenza virus). In all reported PCLTS studies, the model showed reproducibility and the PCLTS had good physiological conditions during the time of the assay [7,12,15]. Recently, PCLTS from sheep were infected with Jaagsiekte sheep retrovirus, the causative agent of ovine pulmonary adenocarcinoma. The virus was able to infect cells, produce new infectious virions, and induce cell proliferation. Also, infected lung slice cells expressed markers of type II pneumocytes and phosphorylated Akt and ERK1/2, resembling the phenotype of natural and experimentally-derived OPA in sheep [7].

A critical factor on PCLTS model is how the tissue is maintained in good physiological conditions to perform the experiments. Previous work in our lab showed that murine PCLTS are viable up to 96 h after obtaining, as monitored by MTT assay and histological studies [19]; all the experiments in this study were done during the first 24 h after infection assuring that PCLTS were suitable to work. Umachandran and colleagues [20], showed that in their conditions rat PCLTS were metabolically viable for 8 h, a short time compared with our murine PCLTS; however, differences may be due to how the tissues were obtained and incubated. Moreover, the rat slice thickness mean was 600 nm, which may limit gas exchange and adequate nutrient flow into the tissue compared to the 450 μm thickness of our slices.

One of the main goals in this work was the optimization to obtain, culture and establish reproducible *M. tuberculosis* infections. Previously, Arriaga et al., [21] detected presence of mycobacterial DNA by PCR *in situ* in macrophages, fibroblasts,

endothelial and bronchial epithelial cells of experimental infected mice after 30 days post-infection, indicating these cells can be infected by *M. tuberculosis*. In the PCLTS we observed bacilli in contact with epithelial cells as well as intracellular bacteria in macrophages. Bacteria were easily located in alveolar space and close or in contact with type II pneumocytes. Although we did not find evidence of intracellular bacteria in these cells, it cannot be discarded cell invasion occurs. Our model analyze early stages of infection up to 48 h and further ultrastructure analysis is needed to confirm infection of pneumocytes in PCLTS. Detailed comparisons of mycobacterial infections in PCLTS to infections by other species may reveal common mechanisms to human infection. The close proximity of mycobacteria to pneumocytes type II in PCLTS may represent a relevant and preferential location to the infection process as it is well known that mycobacteria invade human lung epithelial cells [22–26].

The histological analysis showed, 24 h after *M. tuberculosis* infection, a moderate infiltrate of immune cells into the areas with a higher number of *M. tuberculosis* bacteria. This movement is similar to the increase of lymphocytes and plasmacytic cells in infection areas with respiratory syncytial virus (RSV) and *Chlamydophila pneumoniae* observed by Ebsen et al. [15] in mice PCLTS. Migration of immune cells is a signal that PCLTS remain immunologically active. Henjakovic et al. [27] reported that immunoactive substances such as lipopolysaccharide (LPS), macrophage-activating lipopeptide-2 (MALP-2), interferon-γ (IFNγ), and dexamethasone induced the characteristic responses to these substances in PCLTS. These facts support this model as suitable to test immune responses against pathogens. Further studies on the phenotype of the immune cells in PCLTS will determine what kind of cells interact directly with Mycobacterium. One advantage of this system is the possibility to add exogenous specific immune cell types to the PCLTS and analyze the role of each cell linage during the challenge with microbes.

Therefore, to analyze the ability of PCLTS to respond immunologically we tested the TNF-α induction on PCLTS infected with mycobacteria. *M. bovis* BCG induced a higher amount of TNF-α than *M. tuberculosis* H37Rv, measured by qRT-PCR. Peaks of expression were at 6 h after infection with an increase of 2.62 and 3.38 fold for *M. tuberculosis* and *M. bovis* BCG, respectively. Differences in expression are not due to differential growth of strains as differences in the number of CFU per slice were not statistically significant as shown in Table 1, but due to differential TNF-α induction by the infecting strains. These results agree with those reported by Wong et al. [28] where they found that virulent strains produced a lower induction of TNF-α than non-virulent strains. These findings suggest that virulent strains may inhibit cellular mechanism to evade innate immune response. An example is the suppression of IL-12 production and negative regulation of apoptosis in host macrophages [29–31] which would allow mycobacteria to survive inside the cells protected from immune response, helping further tissue dissemination.

In a report of *ex vivo* human lung tissue infected with *M. tuberculosis*, *M. avium* and *M. abscessus*, Ganbat et al. [32], found macrophages, neutrophils, monocytes, and pneumocytes-II infected with mycobacteria and nuclear alterations resulting in cell death depending on the mycobacterial species used. This system provides a similarity to the original lung microenvironment with its native cell population, orientation, and structural integrity. In comparison, our model provide homogenous tissue size, favoring gas exchange, nutrient availability, and allowing viability of tissue up to 96 h. Also, mycobacterial inoculum used in our experiments is lower and distribution of bacteria is easier due to the size of the PCLTS.

Morphological changes and the induction of TNF-α of PCLTS experimentally infected with mycobacteria suggest this system as an alternative model to study different aspects of tuberculosis pathogenesis under controlled conditions in a closest way to what occurs *in vivo*. Also, the number of animals used by this approach is lower than typical *in vivo* models. The possible use of PCLTS to study immune responses, virulence factor action, or even to test therapeutic agents are some facets to explore in future research.

Acknowledgement

We would like to thank Russell K. Karls for the critical review of the manuscript.

This work was supported by PAICYT-UANL CN 1534-07, FIS-IMSS 2005/1/I/070 FIS/IMSS/PROT/008, INMUNOCANEI-CONACYT 253053. The funders had no role in study design, data collection and analysis, decision to publish, or preparation of the manuscript.

References

[1] World Health Organization. Tuberculosis fact sheet. http://www.who.int/mediacentre/factsheets/fs104/en/; 2016 [Accessed 16.12.20].
[2] Liu R, An L, Liu G, Li X, Tang W, Chen X. Mouse lung slices: an *ex vivo* model for the evaluation of antiviral and anti-inflammatory agents against influenza viruses. Antivir Res 2015;120:101–11. http://dx.doi.org/10.1016/j.antiviral.2015.05.008.
[3] Fisher RL, Smith MS, Hasal SJ, Hasal KS, Gandolfi AJ, Brendel K. The use of human lung slices in toxicology. Hum Exp Toxicol 1994;13:466–71. http://dx.doi.org/10.1177/096032719401300703.
[4] Wohlsen A, Marti C, Vollmer E, Branscheid D, Magnussen H, Becker WM, et al. The early allergic response in small airways of human precision-cut lung slices. Eur Respir J 2003;21:1024–32. http://dx.doi.org/10.1183/09031936.03.00027502.
[5] de Kanter R, Monshouwer M, Meijer DK, Groothuis GM. Precision-cut organ slices as a tool to study toxicity and metabolism of xenobiotics with special reference to non-hepatic tissues. Curr Drug Metab 2002;3:39–59. http://dx.doi.org/10.2174/1389200023338071.
[6] Abd El Rahman S, Winter C, El-Kenawy A, Neumann U, Herrler G. Differential sensitivity of well-differentiated avian respiratory epithelial cells to infection by different strains of infectious bronchitis virus. J Virol 2010;84:8949–52. http://dx.doi.org/10.1128/JVI.00463-10.
[7] Cousens C, Alleaume C, Bijsmans E, Martineau HM, Finlayson J, Dagleish MP, et al. Jaagsiekte sheep retrovirus infection of lung slice cultures. Retrovirology 2015;12:31. http://dx.doi.org/10.1186/s12977-015-0157-5.
[8] Bauer CM, Zavitz CC, Botelho FM, Lambert KN, Brown EG, Mossman KL, et al. Treating viral exacerbations of chronic obstructive pulmonary disease: insights from a mouse model of cigarette smoke and H1N1 influenza infection. PLoS One 2010;5:e13251. http://dx.doi.org/10.1371/journal.pone.0013251.
[9] Meng F, Punyadarsaniya D, Uhlenbruck S, Hennig-Pauka I, Schwegmann-Wessels C, Ren X, et al. Replication characteristics of swine influenza viruses in precision-cut lung slices reflect the virulence properties of the viruses. Vet Res 2013;44:110. http://dx.doi.org/10.1186/1297-9716-44-110.
[10] Dobrescu I, Levast B, Lai K, Delgado-Ortega M, Walker S, Banman S, et al. *In vitro* and *ex vivo* analyses of co-infections with swine influenza and porcine reproductive and respiratory syndrome viruses. Vet Microbiol 2014;169:18–32. http://dx.doi.org/10.1016/j.vetmic.2013.11.037.
[11] Punyadarsaniya D, Liang CH, Winter C, Petersen H, Rautenschlein S, Hennig-Pauka I, et al. Infection of differentiated porcine airway epithelial cells by influenza virus: differential susceptibility to infection by porcine and avian viruses. PLoS One 2011;6(12):e28429. http://dx.doi.org/10.1371/journal.pone.0028429.
[12] Delgado-Ortega M, Melo S, Punyadarsaniya D, Ramé C, Olivier M, Soubieux D, et al. Innate immune response to a H3N2 subtype swine influenza virus in newborn porcine trachea cells, alveolar macrophages, and precision-cut lung slices. Vet Res 2014;45:42. http://dx.doi.org/10.1186/1297-9716-45-42.
[13] Kirchhoff J, Uhlenbruck S, Goris K, Keil GM, Herrler G. Three viruses of the bovine respiratory disease complex apply different strategies to initiate infection. Vet Res 2014;45:20. http://dx.doi.org/10.1186/1297-9716-45-20.
[14] Kirchhoff J, Uhlenbruck S, Keil GM, Schwegmann-Wessels C, Ganter M, Herrler G. Infection of differentiated airway epithelial cells from caprine lungs by viruses of the bovine respiratory disease complex. Vet Microbiol 2014;170:58–64. http://dx.doi.org/10.1016/j.vetmic.2014.01.038.
[15] Ebsen M, Mogilevski G, Anhenn O, Maiworm V, Theegarten D, Scharze J, et al. Infection of murine precision cut lung slices (PCLS) with respiratory syncytial virus (RSV) and *Chalmydophila pneumoniae* using the Krumdieck technique. Pathol Res Pract 2002;198:747–53. http://dx.doi.org/10.1078/0344-0338-00331.
[16] Dassow C, Wiechert L, Martin C, Schumann S, Müller-Newen G, Pack O, et al. Biaxial distension of precision-cut lung slices. J Appl Physiol 2010;108:713–21. http://dx.doi.org/10.1152/japplphysiol.00229.2009.

[17] Castro-Garza J, Barrios-García HB, Cruz-Vega DE, Said-Fernández S, Carranza-Rosales P, Molina-Torres CA, et al. Use of a colorimetric assay to measure differences in cytotoxicity of *Mycobacterium tuberculosis* strains. J Med Microbiol 2007;56:733–7. http://dx.doi.org/10.1099/jmm.0.46915-0.
[18] Harford CG, Hamlin A. Effect of influenza virus on cilia and epithelial cells in the bronchi of mice. J Exp Med 1952;95:173–90. http://dx.doi.org/10.1084/jem.95.2.173.
[19] Jaramillo-Reyna E. Rebanadas de tejidos: un modelo alternativo en investigación biomédica (Undergraduate Thesis). Nuevo León, México: Universidad Autónoma de Nuevo León; 2006.
[20] Umachandran M, Howarth J, Ioannides C. Metabolic and structural viability of precision-cut rat lung slices in culture. Xenobiotica 2004;34:771–80. http://dx.doi.org/10.1080/00498250400000816.
[21] Arriaga AK, Orozco EH, Aguilar LD, Rook GA, Hernández Pando R. Immunological and pathological comparative analysis between experimental latent tuberculous infection and progressive pulmonary tuberculosis. Clin Exp Immunol 2002;128:229–37. http://dx.doi.org/10.1046/j.1365-2249.2002.01832.x.
[22] Hernández-Pando R, Jeyanathan M, Mengistu G, Aguilar D, Orozco H, Harboe M, et al. Persistence of DNA from *Mycobacterium tuberculosis* in superficially normal lung tissue during latent infection. Lancet 2000;356:2133–8. http://dx.doi.org/10.1016/S0140-6736(00)03493-0.
[23] Castro-Garza J, King CH, Swords WE, Quinn FD. Demonstration of spread by *Mycobacterium tuberculosis* bacilli in A549 epithelial cell monolayers. FEMS Microbiol Lett 2002;212:145–9. http://dx.doi.org/10.1111/j.1574-6968.2002.tb11258.x.
[24] García-Pérez BE, Mondragón-Flores R, Luna-Herrera J. Internalization of Mycobacterium tuberculosis by macropinocytosis in non-phagocytic cells. Microb Pathog 2003;35:49–55. http://dx.doi.org/10.1016/S0882-4010(03)00089-5.
[25] García-Pérez BE, Hernández-González JC, García-Nieto S, Luna-Herrera J. Internalization of a non-pathogenic mycobacteria by macropinocytosis in human alveolar epithelial A549 cells. Microb Pathog 2008;45:1–6. http://dx.doi.org/10.1016/j.micpath.2008.01.009.
[26] Rivas-Santiago B, Contreras JC, Sada E, Hernández-Pando R. The potential role of lung epithelial cells and beta-defensins in experimental latent tuberculosis. Scand J Immunol 2008;67:448–52. http://dx.doi.org/10.1111/j.1365-3083.2008.02088.x.
[27] Henjakovic M, Sewald K, Switalla S, Kaiser D, Müller M, Veres TZ, et al. *Ex vivo* testing of immune responses in precision-cut lung slices. Toxicol Appl Pharmacol 2008;231:68–76. http://dx.doi.org/10.1016/j.taap.2008.04.003.
[28] Wong KC, Leong WM, Law HK, Ip KF, Lam JT, Yuen KY, et al. Molecular characterization of clinical isolates of *Mycobacterium tuberculosis* and their association with phenotypic virulence in human macrophages. Clin Vaccine Immunol 2007;14:1279–84. http://dx.doi.org/10.1128/CVI.00190-07.
[29] Nigou J, Gilleron M, Rojas M, Garcia LF, Thurnher M, Puzo G. Mycobacterial lipoarabinomannans: modulators of dendritic cell function and the apoptotic response. Microbes Infect 2002;4:945–53. http://dx.doi.org/10.1016/S1286-4579(02)01621-0.
[30] Deretic V, Singh S, Master S, Harris J, Roberts E, Kyei G, et al. *Mycobacterium tuberculosis* inhibition of phagolysosome biogenesis and autophagy as a host defense mechanism. Cell Microbiol 2006;8:719–27. http://dx.doi.org/10.1111/j.1462-5822.2006.00705.x.
[31] Loeuillet C, Martinon F, Perez C, Munoz M, Thome M, Meylan PR. *Mycobacterium tuberculosis* subverts innate immunity to evade specific effectors. J Immunol 2006;77:6245–55. http://dx.doi.org/10.4049/jimmunol.177.9.6245.
[32] Ganbat D, Seehase S, Richter E, Vollmer E, Reiling N, Fellenberg K, et al. Mycobacteria infect different cell types in the human lung and cause species dependent cellular changes in infected cells. BMC Pulm Med 2016;16:19. http://dx.doi.org/10.1186/s12890-016-0185-5.